JBC Papers in Press. Published on June 14, 2004 as Manuscript M400484200

JBC, submitted Jan 15th, 2004
revised June 8th, 2004

Inhibition of furin by polyarginine-containing peptides: nanomolar inhibition by nona-D-arginine

Magdalena M. Kacprzak[1], Juan R. Peinado[1], Manuel E. Than[2], Jon Appel[3], Stefan Henrich[2], Gregory Lipkind[4], Richard A. Houghten[3], Wolfram Bode[2], and Iris Lindberg[†1*]

[1] Department of Biochemistry and Molecular Biology
Louisiana State University Health Sciences Center, New Orleans, LA 70112
[2] Department of Structural Research, Max-Planck-Institute for Biochemistry,
Am Klopferspitz 18A, 82152 Martinsried, Germany
[3] Torrey Pines Institute for Molecular Studies, San Diego, CA 92121
[4] The University of Chicago, Dept. Biochemistry

Keywords: Furin, inhibitors, polyarginines, proprotein convertase, anthrax, serine protease, subtilase

† To whom correspondence should be addressed:
Iris Lindberg, Ph.D.
Dept. of Biochemistry and Molecular Biology,
Louisiana State University Health Sciences Center
1901 Perdido St., New Orleans, LA 70112
Tel.: 504-568-4799
Fax: 504-568-6598
e-mail: ilindb@lsuhsc.edu.

Abbreviations

α1-PDX, α1-antitrypsin Portland; D6R, hexa-D-arginine; D6K, hexa-D-lysine; D7R, hepta-D-arginine; D8R, octa-D-arginine; D9R, nona-D-arginine; DHFR, dihydrofolate reductase; HIV, human immunodeficiency virus; L6R, hexa-L-arginine; L9R, nona-L-arginine; LF, lethal factor; PA, protective antigen; PC, proprotein/prohormone convertase; pERTKR-MCA, pGlu-Arg-Thr-Lys-Arg-4-methylcoumaryl-7-amide

Summary

Polyarginine-containing peptides represent potent inhibitors of furin, a mammalian endoprotease which plays an important role in metabolism, activation of pathogenic toxins and viral proliferation. The therapeutic use of D-polyarginines is especially interesting since they are not cleaved by furin and possess inhibitory potency almost equal to L-polyarginines. In this study we attempted to determine the important elements within polyarginines which contribute to effective inhibition. Structure-function analyses of polyarginine peptides showed that inhibition by polyarginine-containing peptides appeared to depend on the total number of basic charges of the positively charged inhibitors bound to the negatively charged substrate binding pocket; peptide positioning did not appear to be rigorously determined. Screening of L- and D-decapeptide positional scanning combinatorial peptide libraries indicated a preference for basic residues in nearly all positions, similar to previous results with hexapeptide libraries. Length and terminal modification studies showed that the most potent D-polyarginine tested was D9R amide with a K_i of 1.3 nM. D9R amide was shown to protect RAW264.7 cells against anthrax toxemia with an IC50 of 3.7 μM. Because of its high stability, specificity, low toxicity, small molecular weight, and extremely low K_i against furin, D9R amide or its derivatives may represent promising compounds for therapeutic use.

Introduction

Furin is a mammalian subtilisin/Kex2p-like endoprotease which is involved in the processing of many precursor proteins (reviewed in 1, 2, 3). The enzyme has a ubiquitous tissue distribution and cycles between the trans-Golgi network, the cell surface and the endosomes. Furin plays a role in embryogenesis and homeostasis (4) and is also responsible for processing bacterial toxin precursors and virus envelope glycoprotein precursors (5, 6). Because of its involvement in bacterial and viral pathogenesis, furin represents an attractive target for therapeutic drugs.

Polyarginines are known to be potent, small inhibitors of furin; L6R (hexa-L-arginine), for example, exhibits the low inhibition constant (K_i) of 114 nM (7), and the D-forms of these polyarginines were also shown to be inhibitory. Moreover D6R amide has been shown to block the activation of *Pseudomonas aeruginosa* exotoxin A (8) and to protect against anthrax toxemia both *in vivo* and *in vitro* (9).

The structure of mouse furin has been recently determined (10) and reveals that the enzyme's active site contains an extended substrate-binding groove which is lined with many negatively charged residues: these include D258 and D306 (surrounding the S1 subsite); D154 and D191, which form the surface of the S2 pocket; E236 and E264 (S4 subsite); E257 and D264 (D264 takes part in forming the S4 and S5 subsites); and E230 and D233 (S6 subsite). No basic residues are present in the general area between the S5 and S1 subsites; basic residues (R193, H364 and R197) are found only on the outer edge of the S1' subsite. The highly acidic character of the substrate-binding groove explains the high inhibitory potency of positively charged polyarginine-containing peptides.

In the work described here we present the further study of the inhibitory features of polyarginines against human furin. We attempted to gain information on the positioning of D6R amide within the furin substrate binding pocket. We also scanned decapeptide libraries in search of a highly inhibitory sequence, and tested how length and terminal modification can influence the inhibitory potency of D-arginine-containing peptides.

Materials and Methods

Materials – The positional scanning decapeptide libraries and other peptides were synthesized at the Torrey Pines Institute for Molecular Studies (San Diego, CA). If not stated otherwise, all peptides were carboxy-terminally amidated, with free amino termini. The

decapeptide library consisted of 200 L- or D- peptide mixtures, divided into ten groups corresponding to each position within the decapeptide. For each position, 20 mixtures were surveyed, each of which was defined by one of the 20 natural amino acids. The undefined positions were occupied by any of the amino acids except cysteine. The positional scanning library and the individual compounds were synthesized using simultaneous multiple peptide synthesis methodology as described previously (7).

Concentration of peptides – Although the peptides used in this study were over 99% pure, these highly basic peptides consisted of more than half salt (trifluoroacetate) and water; the actual molar concentration was thus smaller than expected. The amount of peptide in each stock was determined by quantitative amino acid analysis at the Microchemical Facility at the Winship Cancer Institute (Atlanta, GA). Using amino acid analysis, D6R amide, D7R amide, D8R amide and D9R amide were shown to contain 36%, 36%, 48% and 31% (w/w) respectively of actual peptide. Unless otherwise stated (in the figure legends) we here report peptide concentrations taking the required correction into account. Where the actual amino acid composition is not known (i. e. the peptides described in **Figure 2** and **Figure 5**), this correction has not been made.

Human furin preparation – The pCMV-Fur_S vector containing cDNA encoding truncated human furin was obtained from J. W. Creemers (11). CHO K1 cells were stably transfected and expression amplified using the DHFR-coupled amplification method as described previously (12). The method described for mouse furin purification (7) was used for purification of human furin from conditioned media.

PACE4 preparation – Conditioned medium containing PACE4 was obtained from stably transfected HEK293 cells (13) as described previously (7). One liter of medium was diluted three times with buffer A (20 mM HEPES pH 7.4, 0.1% Brij 35), loaded on a 5 ml Econo-Pac® anion exchange cartridge (Bio-Rad), and eluted using a linear gradient of 0- 0.5 M NaCl in 45 min. The flow rate was 1 ml/min and 1 ml fractions were collected.

Enzyme assays – The assay for furin was performed at pH 7.0 in 100 mM HEPES, 5 mM CaCl2, and 0.1% Brij 35. The substrate and enzyme concentration unless otherwise stated were 200 μM and 15 nM, and the total assay volume was 50 μl. Inhibitory peptides were preincubated with enzyme for 30 min at 37°C prior to addition of substrate. All assays were performed either in duplicate or triplicate. Inhibition constants were determined as in (14) and the equation $K_i = K_{i(app)} / (1 + ([S]/K_m))$ was used. The K_m value of the substrate pERTKR-methylaminocoumarin

(pERTKR-MCA) for human furin was 5 μM, as determined by kinetic analysis (Prism GraphPad software).

Decapeptide scanning analysis – The decapeptide libraries were tested for furin inhibition, and the data for each sample in each experiment were normalized as follows. An absolute value (x_1) representing the percent of furin inhibition was calculated for each peptide mixture of the library (all negative values of inhibition were taken as zero). Then absolute values of all peptide mixtures for a given position were summed (x_{total}), and the arbitrary percentage value x_2 for the particular amino acid were calculated (where $x_2 = [x_1/x_{total}] * 100\%$). For example, if we observe 95% inhibition of enzyme activity caused by a peptide mixture having arginine defined in the fifth position (R5), and no other residue in the fifth position is inhibitory, the peptide mixture exhibits 100% participation in overall inhibition ($x_2 = 100\%$). If in the seventh position we observe 99% inhibition by a peptide mixture defined by arginine, 99% inhibition by lysine, and 5% inhibition of alanine, we calculate that the peptide mixture defined with arginine in the seventh position (R7) creates 48.8% of total inhibition, because 99/[99+99+5] * 100% = 48.8%. Following this normalization, the means from five independent experiments could be calculated.

Cell culture and cytotoxicity assay – The inhibitory effect of D6R amide and D9R amide on anthrax toxemia was studied in RAW264.7 cells. RAW cells were cultured at 10^4/well in a 96 well flat-bottomed plate (Costar) and treated 12 h later with 400 ng/ml protective antigen (PA; obtained from S. Leppla, NIH) and 200 ng/ml lethal factor (LF; obtained from S. Leppla, NIH) in the presence of 1 to 15 μM polyarginine, for 1 h. Each condition was examined in triplicate. The inhibitors were added immediately after addition of PA+LF (i.e. anthrax toxin, AT). All experiments were repeated independently two times and the results are expressed as mean ±SEM of the triplicates. Cell growth was monitored with the compound WST-1 (Roche Diagnostics) using the manufacturer's protocol; this assay reflects the activity of mitochondrial dehydrogenase present in living cells. When applied alone at 100 μM, D9R amide, like D6R amide (9) did not produce any cytotoxic effects on RAW cell growth (J. R. Peinado, data not shown).

Inhibitor modeling studies – The crystal structure of mouse furin inhibited with a decanoyl-RVKR-chloromethylketone inhibitor (10) was used for all modeling studies. This structure is also representative of human furin, since all amino acid residues within the active-site cleft are conserved. The (L)-RRRRRRDL - peptide was manually placed into the active-site cleft considering i) the experimentally defined interactions between the P4 through P1 inhibitor side

chains with the corresponding S4 through S1 proteinase subsites; ii) the structure of the subtilisin / eglin c complex (15); and iii) the subtilisin BPN'-prodomain complex (16). The initial model for the retro binding of the (D)-ldrrrrrr peptide was constructed from this L-peptide by superimposing all C^{α} and side chain atoms following reversal of the polypeptide chain (simple retro binding); this however resulted in poor carbonyl-carbonyl contacts between the inhibitor and furin. For a second starting model, these poor main chain-main chain contacts were manually relieved by a 180° flipping of the inhibitor peptide groups (retro binding with flipping). In addition, this flipping reestablished favorable inter-main chain hydrogen bonds, but required some C^{α} and side chain shifts to maintain favorable intermolecular peptide geometries. In the third model, the (D)-rrrrrrdl peptide was manually placed into the active-site cleft in a direct binding mode, with optimization of all hydrogen bond and noncovalent interactions between inhibitor and enzyme. The intramolecular energy of these model peptides was minimized by MAIN (17) using the Engh and Huber parameters (18) for bond length, bond angles, dihedral angles and improper angles. The models obtained were subsequently optimized against the fixed furin structure by molecular mechanics using the module DISCOVER (version 2.95) of INSIGHT II (version 2000, Molecular Simulations Inc., San Diego, CA), resulting in the conformations shown in **Figure 1**. Energy minimization was done *in vacuo* using a dielectric constant of 10 and a consistent valence force-field (19) regarding charges, cross and Morse terms. After 10,000 refinement steps of the steepest descent method, a maximum derivative of the energy term of < 1.0 kcal mol^{-1} $Å^{-1}$ was reached.

Results

Determination of the position of D6R amide in the substrate binding pocket – There are in principle two potential directionalities for the binding of the D- peptide inhibitors. They can bind somewhat similar to L-amino acid substrates, i.e. with the N-terminal end of the peptide directed toward the S5, S6 enzyme pocket subsites and the C-terminal end placed close to the S1' S2' subsites. However, due to the distinct stereochemistry at most of the subsites, in particular at S1, the (D)-arginine side chains cannot be optimally accommodated in the subsites with the simultaneous formation of favorable main chain-main chain interactions. It is also possible that D-peptides bind in the reverse direction.

The crystal structure of furin (10) shows a positively charged area at the edge of the S1' specificity pocket formed by R193, H364 and R197 (**Figure 1**). We speculated that this positively charged area could potentially anchor a D6R peptide containing terminal acidic residues. This anchor could provide information about peptide orientation as well as possibly increase inhibitory potency. We synthesized amidated (D)-rrrrrr (D6R) and (D)-rrrr (D4R) peptides containing (D)-dl and (D)-el at either the N or C termini and assayed these for inhibition of furin. Calculated K_is are presented in **Figure 2**. In all cases the addition of negatively charged residues led to an increase in K_is. The addition of (D)-el and (D)-dl to D4R led to 30- and 120-fold increase in K_is The addition of (D)-dl and (D)-el to D6R amide caused a several-fold increase in K_i (see **Figure 2**). In all cases we observed that the addition of glutamate was worse for inhibitory potency than the addition of aspartate residue. Furthermore, we observed a slight but significant relationship in that acidic residues added to the carboxy terminus represented more potent inhibitors than those which contained acidic residues on the amino terminus, suggesting that these peptides may indeed favor an orientation in which the acidic residues bind to the positively charged area at the end of the acidic groove, i.e. in the same direction as L-peptides/substrates. Alternatively, since the difference between (D)-ldrrrrrr and (D)-rrrrrrdl (and the glutamic acid pair) is quite small, it could simply be due to their use of different registries for binding (see below). In summary, the addition of potentially "anchoring" acidic residues did not improve binding ability over the starting compound D6R amide; any change in overall charge did, however, diminish binding affinity.

In order to determine how D-polyarginines bind to the furin substrate binding pocket, we tested modified D6R amide peptides, in which each position was sequentially substituted by either alanine or lysine. Since the furin cleavage consensus sequence is RXR/KR (reviewed in 1), we expected to find D6R amide binding directly into the acidic groove in any position between the S6 and S3' sites. However, as discussed below, the positional scanning library results did not support a specific positioning of D6R amide in the acidic substrate pocket.

Positioning of the hexapeptide from S6 toward the S1 site (S6→S1, see scheme in **Figure 2** showing theoretical positioning) was judged to be unlikely because lysine substitution in the (L)-rrrrrk peptide or alanine in the (L)-rrrrra peptide would then be located in the S1 site, which should lead to an unfavorably large increase in K_i (this site strictly requires arginine; (1)).

However, as shown in **Figure 2**, we observed only slightly increased K_is for these two peptides as compared to (D)-rrrrrr (D6R). S5→S1' positioning also appeared unlikely, because in this case the alanine within the peptide (D)-rrrarr would be located in the S2 site (also known to prefer arginine or lysine), and therefore this positioning would not be associated with the relatively low K_i we observed. The S4→S2' positioning of the hexapeptides was also judged unlikely, because the peptide (D)-rrrarr with alanine at the presumed S1 site should be a much worse inhibitor than D6R amide; however, we found that this peptide still exhibited a relatively good K_i. Moreover, the very large increase in K_i observed with the (D)-rrkrrr peptide (where lysine is placed in the well-accepting S2 site) also should not have been obtained if the peptide is placed in the position S4→S2'.

In the above analysis we assumed that D6R amide is oriented similarly to substrates. Since it is equally possible that the peptides bind in a reverse orientation (see above), we performed a similar analysis for the reverse orientation. This brought us to a similar conclusion, i.e. that no specific positioning is favored. Summarizing, from this experiment we conclude that the various polyarginine-containing peptides most likely do not always bind in the same orientation into the sub-pockets, but may adopt various binding configurations depending on the specific peptide.

Modeling studies of D-peptides into the furin substrate binding pocket – In order to obtain views of the possible modes of D-peptide binding, we modeled different D- and L-peptides into the active-site cleft of furin (**Figure 1**). Starting from the experimentally observed covalent binding of the tetrapeptide (L)-RVKR to the active site (10), we exchanged all residues with arginine residues, added a P6 and a P5 arginine residue at the N-terminus and extended the C-terminus by aspartic acid or glutamic acid at P1' and leucine at P2'. Energy minimization of the resulting L-peptide-complexes with MAIN and DISCOVER validated this methodology and clearly showed the location of the P5, P6 and P1' and P2' residues in the corresponding subsites (**Figure 1 A, B**). The furin residues R193, H364 and R197, located at the border of the S1' pocket provide (in strong contrast to the non-prime subsites) a positive electrostatic surface potential, which should attract negatively charged side chains such as glutamic acid and aspartic acid, in agreement with the known substrate profile of furin. While the P6 to P1 residues remained mostly unchanged during refinement with DISCOVER, the primed-side residues

moved slightly away from the surface, obviously due to unfavorable interference with the rigid furin structure (**Figure 1B**).

Modeling of the D-polyarginine peptides did not reveal a clearly preferred binding geometry. Upon direct binding, favorable inter-main chain hydrogen bonds remain possible, with most side chains, in particular those of the P1 and the P2 residue, requiring some rearrangement (**Figure 1C**). Upon simple retro binding, all main and side chain atoms in principle can superimpose with the equivalent residues of the experimental L-peptide structure, resulting, however, in the loss of inter-main chain hydrogen bonds and in bad contacts between the P1-carbonyl and the carbonyl-oxygen of S253 (2.0 A), and the P3-carbonyl and the carbonyl-oxygen of G255 (1.8 A; data not shown). We attempted to relieve these poor contacts by molecular mechanics calculations before (**Figure 1D**) or after (**Figure 1E**) manual flipping of the peptide bonds of the inhibitor. A comparison of these models with the initial L-peptide model (thin, gray stick models in Figure 1) shows that the three D-peptide models exhibit reasonable binding geometries, with good intermolecular energies of the inhibitor and reasonable interactions between the inhibitor and the enzyme surface. With the D-peptides, however, it is not possible to simultaneously satisfy all side chain and main chain interaction requirements available to the L-peptides. This is in agreement with our experimental results, described below, showing that poly-L-arginines exhibit a higher affinity than poly-D-arginines. Due to the many detailed differences observed, the energies resulting from energy minimization of the D-peptides are not directly comparable. We therefore conclude from our modeling studies that several binding geometries seem to be possible for D-peptides and that a ranking of these possibilities is not feasible.

L- and D- decapeptide library scanning – In order to identify a potent inhibitory decapeptide sequence, we screened positional scanning carboxy - terminally amidated L- and D-decapeptide libraries. The libraries were tested five times with various concentrations of substrate (from 100 μM to 200 μM pERTKR-MCA), of the inhibitory library (from 0.6 mg/ml to 1 mg/ml); and of the enzyme (from 25 nM to 100 nM). In all cases the pattern of inhibition was similar, showing differences only in the level of discrimination. In each experiment, for each position we have calculated the inhibitory contribution of a particular peptide mixture defined with an amino acid in comparison with other peptide mixtures (see *Materials and Methods*). The mean values from five experiments, representing the percent contributions of the defined amino acid in overall

inhibition for a given site, were calculated. **Figure 3** shows that basic residues are greatly preferred in almost all positions of the both D- and L- decapeptides.

In three N-terminal positions of the L-decapeptide library the most preferred residue is lysine (18, 27, 18 % respectively), just ahead of arginine (16, 18, 17%). Similarly in the fourth and fifth positions arginine (24 and 25%) and lysine (22 and 22%) were the most potent. In the sixth position of the L-decapeptide library threonine-containing peptides (19%) appeared to be slightly better inhibitors than those containing arginine (19%) or serine (13%). The most potent C-terminus therefore favored the sequence: (L)-HRRH (28%, 40%, 42%, and 37%). Library screening also revealed that glutamic acid and aspartic acid, but also other amino acids such as proline, tyrosine, tryptophan, and to a lesser extent alanine, cytosine, glutamine, asparagine, and glycine were not well accepted at any position. Methionine residues at the third, sixth, and tenth positions were much better tolerated than at other positions. Leucine, valine, and isoleucine residues appeared to be neutral with regard to effects on inhibitory potency.

Scanning of the D-decapeptide library showed, however, a different and somewhat puzzling pattern of inhibitory potency. Arginine was the most inhibitory residue in almost every position, but was most essential in the second and third positions. D-lysine in positions 1 to 5 exhibited good inhibition, and (in contrast to the L-decapeptide library screening) was also acceptable in the eighth position. Interestingly, histidine was not inhibitory in any position. Also in contrast to the L-peptide library screening, the presence of glutamic acid in the seventh and ninth positions of the D-decapeptide library was moderately inhibitory. D-decapeptides containing valine in the fourth position also exhibited substantial inhibition.

Polyarginine characterization – It has been previously shown that L9R, even though it can be cleaved by furin, was significantly more potent an inhibitor than both D6R-amide and L6R (7). We therefore tested the inhibitory potency of D-polyarginines of different lengths against human furin. D-peptides were not cleaved by furin (data not shown).

Similar to previous results obtained using L-peptides (7), an increase in chain length led to a decrease of K_i, yielding in the case of D9R-amide the extremely low K_i of 1.3 nM ± 0.2 (**Figure 4**). Surprisingly, carboxy-terminal amidation lowered the K_i of D6R eight times below that of the unmodified form (**Figure 5**). A detailed examination of the various unmodified and amidated forms of L6R and L9R supported the idea that carboxy-terminal amidation decreases the

inhibitory potency of L-peptides but increases it in the case of D-peptides. We also tested the inhibitory potency of other basic peptides. D6K (D-hexalysine) amide did not exhibit inhibitory potency against furin; the K_i of this peptide was over 15 μM (data not shown).

We examined also the K_i of D6R amide in buffers of different ionic strength. We show that a two-fold increase in ionic strength leads to a two-fold decrease in D6R amide potency (**Table 1)**. The K_m of pERTKR- MCA is simultaneously affected; in buffers of higher ionic strength, the Michaelis constant increased. The calculated K_i of D6R amide is lower than 3 nM in a 50 mM buffer, while it increases to over 25 nM in 200 mM HEPES.

The inhibitory effect of D9R was also tested against PC1, PC2, and PACE4. The activity of PC1 and PC2 was not affected by D9R, while the K_i of D9R against PACE4 was greater than 25 μM.

Protection of anthrax toxemia by D9R amide in RAW264.7 cells - Previous studies showed that the D6R amide prevents anthrax toxemia in RAW cells by inhibiting PA cleavage (9). Because D9R amide exhibited a better K_i for furin in enzymatic assays, we tested whether this nonamer is also more potent in blocking anthrax toxemia (**Figure 6**). At every concentration (from 1 μM to 15 μM) D9R amide exhibited improved protection of cells treated with anthrax toxin over D6R amide. We estimated the IC50 to be 3.7 μM. Even at a 1 μM concentration, at which D6R amide was not effective against anthrax toxin, D9R amide treatment resulted in cellular survival of approximately 30%. We also observed that concentrations of D9R amide as high as 250 μM were not toxic (data not shown).

Discussion

In our previous study (7) we found that polyarginine-containing peptides represent potent inhibitors of mouse furin. Since furin is known to take part in activation of several bacterial and viral propeptides or glycoprotein precursors such as the Ebola virus glycoprotein (5), the HIV envelope glycoprotein (6), *Pseudomonas aeruginosa* exotoxin A (20), diphtheria toxin (21), and anthrax toxin (2), these inhibitors may have an eventual therapeutic application. The most potent polyarginine-containing peptide previously identified was nona-L-arginine, having a K_i of 42 nM (7). The peptide was however cleaved by furin, yielding shorter peptides which still retained inhibitory activity. Interesting was the fact that the unnatural D-form of hexa-arginine was almost as inhibitory as the L-form, having a K_i of 106 nM for mouse furin. In the present study we attempted to learn further about the interaction of furin with polyarginine-containing peptides, as well as to possibly identify a more potent inhibitor with a similar structure.

In order to assign relative importance to the different positions within D6R amide, we performed alanine and lysine scans. Our data however indicate that D-arginine-containing peptides most likely do not bind into the substrate-binding pocket in one strictly determined position; each peptide most likely adopts a different distribution among the minimal energy states available.

It is likely that D-polyarginines bind to the furin substrate binding pocket in a reverse manner. This is suggested by the general observation that lysine substitution at any of the first three positions within D6R amide was not well tolerated. The idea that lysine residues are not tolerated near the S1, S1' sites is also supported by the L-decapeptide library scanning results, which showed that lysine is well accepted only in the N-terminal region of the L-peptides studied. The D-decapeptide library data, however, did not show a similar correlation, which might result from the diversified positioning of D-peptides with respect to the S1-S1' subsites. The fact that amidated D-peptides are more potent than unmodified peptides could also represent an argument for reverse binding, since their non-negatively charged C-termini might exhibit improved binding to the negatively charged non-prime (i.e. from S1 to S6) binding pockets.

On the other hand, with regard to the acidic residue-containing D-polyarginines, these peptides may be oriented normally rather than in a reverse fashion because acidic residues were

somewhat better tolerated when placed on the C-terminus (located near a positively charged area within the enzyme). However, since the K_i differences between (D)-ldrrrrrr and (D)-rrrrrrdl (and the other pair containing glutamic acid) were quite small, they could simply be due to use of different binding registries. Nonetheless, the modeling studies also seem to suggest the D-arginine-containing peptides can bind both in a normal as well as in a reverse manner depending on the particular peptide.

The mechanism of D-polyarginine peptide binding may be mainly based on electrostatic interactions of basic arginines with the negatively charged furin substrate binding groove. This agrees with the observation that higher ionic strength buffers increase the K_i of D6R amide. Reducing the total overall positive charge through the addition of one acidic residue to D6R amide resulted in a 4- to 7.5- fold increase in the K_i. Similarly to previous observations with a hexapeptide library, the positional scanning of the decapeptide libraries (7) showed that basic residues were preferred at all positions. Our data indicate however that charge is not the only element decisive for strong binding into the furin substrate binding pocket, since another basic peptide, D6K amide, exhibited a K_i over three orders of magnitude higher than polyarginines. Similarly we observed that every substitution of D-arginine with D-lysine caused an increase in K_i.

A natural inhibitor for furin has not yet been identified, but the presence of potent natural inhibitors for PC1 (proSAAS; (22)) and PC2 (7B2; (23)) suggests that such a protein may exist. The positional scanning library results can be used to search existing protein sequence databases to predict and identify peptide sequences which may potentially interact with furin *in vivo*. These proteins will be expected to contain an extended highly basic region, a signal peptide, and cellular and tissue distributions consistent with current information on furin.

One of the goals of this study was to identify a more potent polyarginine than D6R amide. We found that the inhibitory potency of D-polyarginines was directly proportional to polyarginine length, similarly to what was earlier shown for L-peptides (7). An interesting observation is that the K_is of D6R amide and D7R amide do not differ significantly from each other, but do differ from the K_is of D8R amide and D9R amide, which are both in turn also

similar. The modification of the peptide ends also appears to contribute to this interaction. In agreement with our present results showing that L-polyarginines were about two times less potent when amidated, acetylation of the N-terminus and amidation of the C-terminus were both previously shown to decrease inhibition of furin by the proSAAS-related peptide 'LLRVKR' (7). However the findings presented here indicate that C-terminal amidation of D-polyarginines enhanced inhibition. These findings suggest that differences exist between the modes of binding of D- and L- peptides. It is interesting that these relatively small modifications of terminal ends can produce relatively large changes in K_i. This feature may be of interest for the introduction of further modifications which could produce yet more potent inhibitors.

In summary, we here report a new, highly potent furin inhibitor, D9R amide with the low K_i of 1.3 nM. While other quite potent furin inhibitors have been recently reported, such as α1-antitrypsin Portland (K_i of 600 pM; (24)), and modified eglin c (K_i of 310 pM; (25)), the former inhibitor possesses a fairly large molecular weight which makes it a difficult therapeutic, while the latter inhibitor represents only a temporary inhibitor of furin. D9R amide on the other hand is stable, relatively small, and easily synthesized. The efficacy of this nonapeptide against anthrax toxemia in RAW cells suggests that this compound or its derivatives may represent promising candidate inhibitors for therapeutic use.

Acknowledgments: This work was supported by NIH grant AI 53517-02 and by the DFG grants SFB596 and TH 862/1-1 to I.L. and a Junta de Andalucia grant to J.R.P. We thank S. Leppla for the protective antigen and lethal factor used in this study.

References

1. Nakayama, K. (1997) *Biochem J* **327 (Pt 3),** 625-35

2. Molloy, S. S., Bresnahan, P. A., Leppla, S. H., Klimpel, K. R., and Thomas, G. (1992) *J. Biol. Chem.* **267,** 16396-16402

3. Thomas, G. (2002) *Nat Rev Mol Cell Biol* **3,** 753-66

4. Roebroek, A. J., Umans, L., Pauli, I. G., Robertson, E. J., van Leuven, F., Van de Ven, W. J., and Constam, D. B. (1998) *Development* **125,** 4863-4876

5. Volchkov, V., Feldmann, H., Volchkova, V. A., and Klenk, H. D. (1998) *Proc. Natl. Acad. Sci. USA* **95,** 5762-5767

6. Hallenberger, S., Bosch, V., Angliker, H., Shaw, E., Klenk, H. D., and Garten, W. (1992) *Nature* **360,** 358-61

7. Cameron, A., Appel, J., Houghten, R. A., and Lindberg, I. (2000) *J Biol Chem* **275,** 36741-9

8. Sarac, M. S., Cameron, A., and Lindberg, I. (2002) *Infect Immun* **70,** 7136-9

9. Sarac, M. S., Peinado, J. R., Leppla, S. H., and Lindberg, I. (2003) *Infection and Immunity* **72,** 602-5

10. Henrich, S., Cameron, A., Bourenkov, G. P., Kiefersauer, R., Huber, R., Lindberg, I., Bode, W., and Than, M. E. (2003) *Nat Struct Biol* **10,** 520-6

11. Ayoubi, T. A., Creemers, J. W., Roebroek, A. J., and Van de Ven, W. J. (1994) *J Biol Chem* **269,** 9298-303

12. Lindberg, I. and Zhou, Y. (1995) Overexpression of neuropeptide precursors and processing enzymes. *Methods in Neuroscience*, Academic Press, Orlando, FL.

13. Mains, R. E., Berard, C. A., Denault, J. B., Zhou, A., Johnson, R. C., and Leduc, R. (1997) *Biochem J* **321 (Pt 3),** 587-93

14. Apletalina, E., Appel, J., Lamango, N. S., Houghten, R. A., and Lindberg, I. (1998) *J Biol Chem* **273,** 26589-95

15. Bode, W., Papamokos, E., and Musil, D. (1987) *Eur J Biochem* **166,** 673-92

16. Gallagher, T., Gilliland, G., Wang, L., and Bryan, P. (1995) *Structure* **3,** 907-14

17. Turk, D. Weiterentwicklung eines Programmes fuer Molekuelgrafik und seine Andwendung auf verschiendene Protein-Strukturaufklaerungen. (1992) Technische Universitaet Muenchen, Germany.

18. Engh, R. A. and Huber, R. (1991) *Acta Cryst* **A43,** 392-400

19. Dauber-Osguthorpe, P., Roberts, V. A., Osguthorpe, D. J., Wolff, J., Genest, M., and Hagler, A. T. (1988) *Proteins* **4,** 31-47

20. Chiron, M., Fryling, C., and FitzGerald, D. (1997) *The Journal of Biological Chemistry* **272,** 31707-31711

21. Tsuneoka, M., Nakayama, K., Hatsuzawa, K., Komada, M., Kitamura, N., and Mekada, E. (1993) *J Biol Chem* **268,** 26461-5

22. Fortenberry, Y., Hwang, J. R., Apletalina, E. V., and Lindberg, I. (2002) *J Biol Chem* **277,** 5175-86

23. Fortenberry, Y., Liu, J., and Lindberg, I. (1999) *J Neurochem* **73,** 994-1003

24. Jean, F., Stella, K., Thomas, L., Liu, G., Xiang, Y., Reason, A. J., and Thomas, G. (1998) *Proc Natl Acad Sci U S A* **95,** 7293-8

25. Komiyama, T., VanderLugt, B., Fugere, M., Day, R., Kaufman, R. J., and Fuller, R. S. (2003) *Proc Natl Acad Sci U S A* **100,** 8205-10

26. Nicholls, A. , Bharadwaj, R., and Honig, B. (1993) *Biophys. J.* **64,** A166

27. Kraulis, P. J. (1991) *J. Appl. Cryst.* **24,** 946-950

28. Merritt, E. A. and Bacon, D. J. (1997) *Methods Enzymol.* **24,** 946-950

29. Schechter, I. and Berger, A. (1967) *Biochem Biophys Res Commun* **27,** 157-62

Figure Legends

Fig. 1. Stereo representation of various potential binding modes of D6R-based inhibitors. The modeled peptides are shown in ball-and-stick-representation (dark gray carbons, blue nitrogens, red oxygens) in front of the solid surface of the active-site cleft of furin colored according to its calculated negative (red -27 e/kT) and positive (blue 27 e/kT) electrostatic surface potential. The (L)-rrrrrrdl peptide was modeled based on an experimental inhibitor structure (10), and its intramolecular energy was minimized in MAIN (panel A and gray stick-representation of panels B-E). The binding mode of this model to the active-site cleft was further optimized using molecular mechanistics calculations in DISCOVER (panel B). The direct binding (D)-rrrrrrdl (panel C) and the retro binding (D)-ldrrrrrr (panels D and E) peptides were minimized in a similar fashion using both MAIN and DISCOVER after manually docking them in direct (N→C) binding mode (panel C), simple retro (C→N) binding mode (i.e., without any further manual interventions, panel D) and in retro binding mode after manual removal of poor contacts by flipping of the peptide bonds (panel E). For further details please refer to the *Materials and Methods* section.

For all models shown, note the proposed electrostatic interaction between aspartic acid - P1' and the positive surface patch formed by R193 and R197, potentially locking the peptides in the registry shown. For easy comparison, all panels are in the same orientation. The inhibitor side chains as well as key residues of importance for the binding properties of the active site cleft are labeled in panel A. This figure was made with Grasp (26), Molscript (27) and Raster3D (28).

Fig. 2. Inhibition constants for various D6R amide-based peptides against furin. The rate of hydrolysis of pERTKR-MCA was determined in the presence of various concentrations of the peptides (each in duplicate or triplicate) as described in *Materials and Methods*. Each K_i value (depicted above the bar) is the mean determined from at least four independent experiments. SDs are represented as error bars. These values do not take into consideration the actual amino acid composition (see *Materials and Methods*). Differences between (D)-lerrrrrr *vs*. (D)-rrrrrrleand (D)-derrrrrr *vs*. (D)-rrrrrrdl are statistically significant ($P<0.05$). Right panel: schematic representation of the furin substrate binding site (nomenclature as per reference 29), depicting the furin cleavage consensus sequence and the possible binding registries of D6R amide.

Fig. 3. Inhibitory potency of the L- and D- decapeptide libraries. The graph represents averaged results from five independent library scans (performed with different concentrations of substrate, enzyme, and inhibitor) and normalized as described in the *Materials and Methods*. Numbers (1-10) represent a defined position in the peptide (counting from the N-terminus). Letters correspond to the defined amino acid. The height of the cone represents the total inhibition of furin by the given amino acid (for details see text). Samples crossed out were not present in the library.

Fig. 4. Inhibition constants for D-polyarginine amides of different lengths against furin. The rate of hydrolysis of pERTKR-MCA was determined in the presence of various concentrations of the peptides (each in duplicate or triplicate) as described in *Materials and Methods*. Each K_i value is the mean ± S.D., determined from at least four independent experiments.

Fig. 5. Inhibition constants for polyarginines with different C-terminal modifications against furin. The rate of hydrolysis of pERTKR-MCA was determined in the presence of various concentrations of the peptides (each in duplicate or triplicate) as described in *Materials and Methods*. Each K_i value (depicted above the bar) is the mean ± S.D. (represented as error bars), determined from four independent experiments. The values do not take into consideration the actual amino acid content (see *Materials and Methods*).

Fig. 6. Protection of RAW cells from anthrax toxemia by D6R amide and D9R amide. Cells were treated with anthrax toxin as described in *Materials and Methods*. Bars represent the percent of surviving cells after treatment with the given concentration of D6R amide and D9R amide, calculated from triplicates. The experiment was repeated twice with similar results.

Table 1

Kacprzak et al., 2004

Table 1. Furin interactions with substrate and inhibitors are dependent upon ionic strength.

	K_m of pERTKR-MCA (μM)	K_i apparent of D6R (μM)	K_i of D6R (nM)
50 mM HEPES	2.9 ± 0.1	0.16 ± 0.01	2.7
100 mM HEPES	4.9 ± 0.2	0.27 ± 0.01	6.5
200 mM HEPES	9.2 ± 0.5	0.62 ± 0.05	26.4

Values represent means ± SE of three independent experiments.

Figure 1

Kacprzak et al., 2004

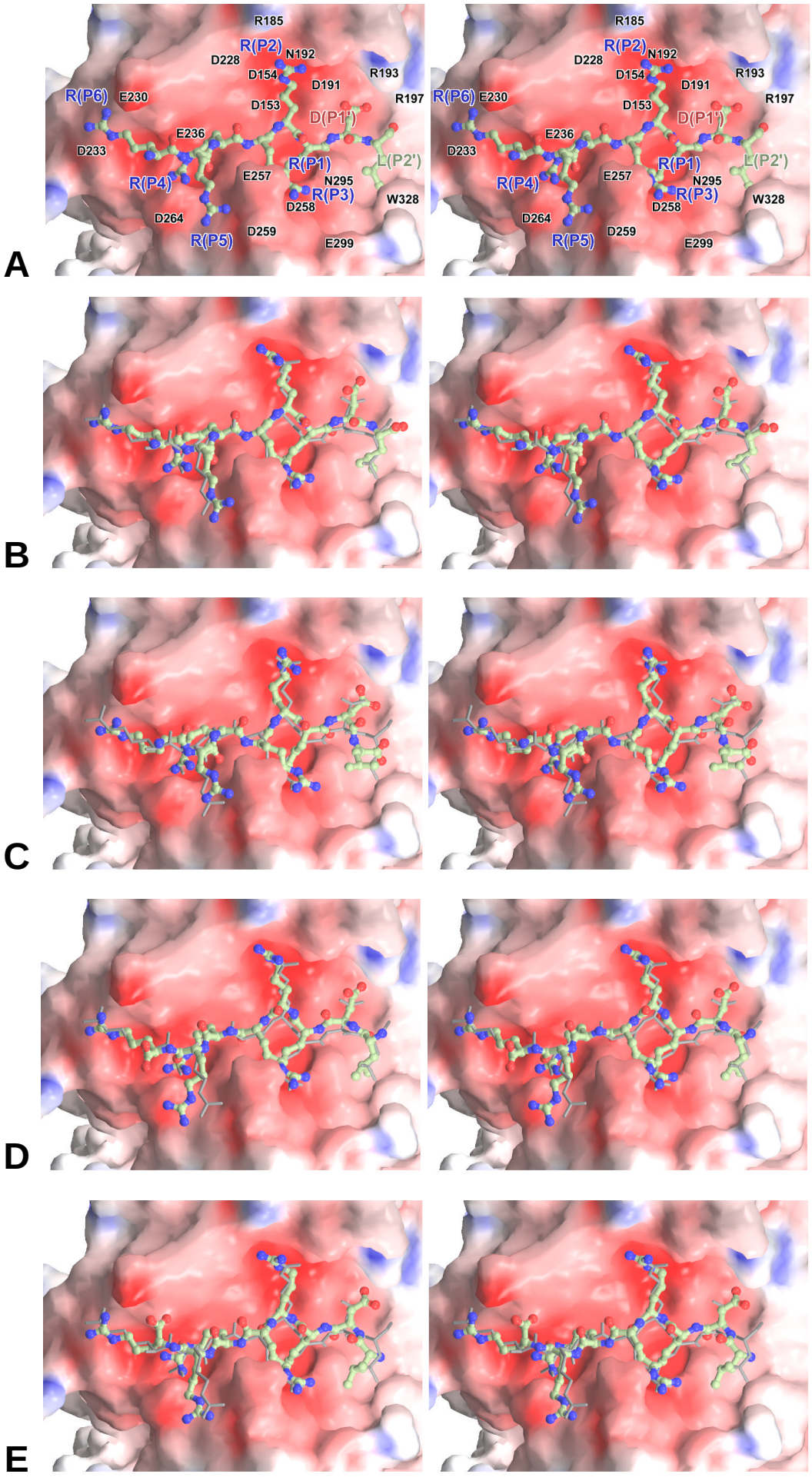

Figure 2

Kacprzak et al., 2004

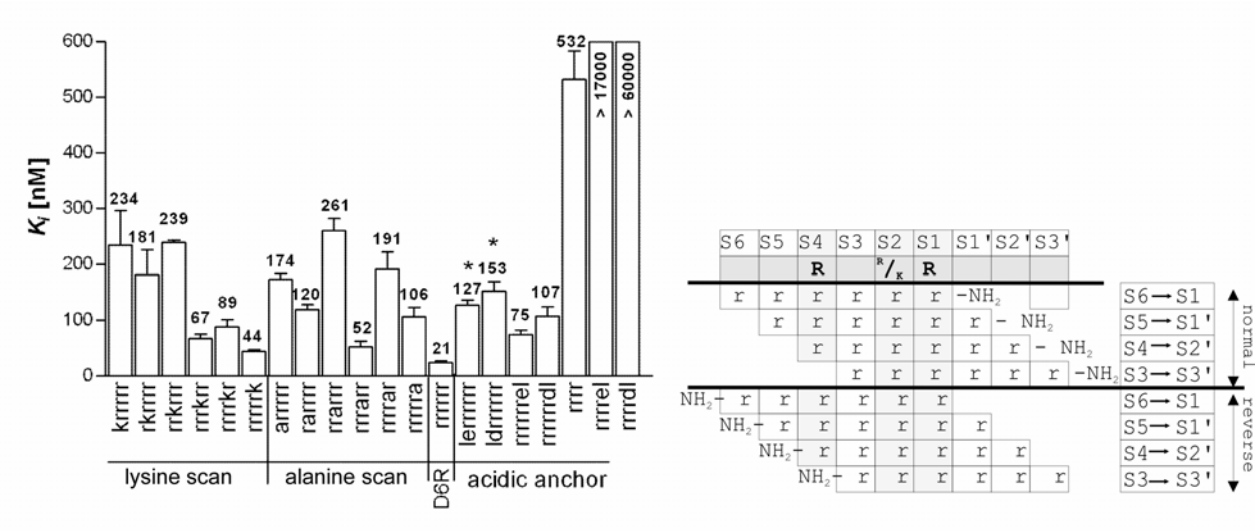

Figure 3

Kacprzak et al., 2004

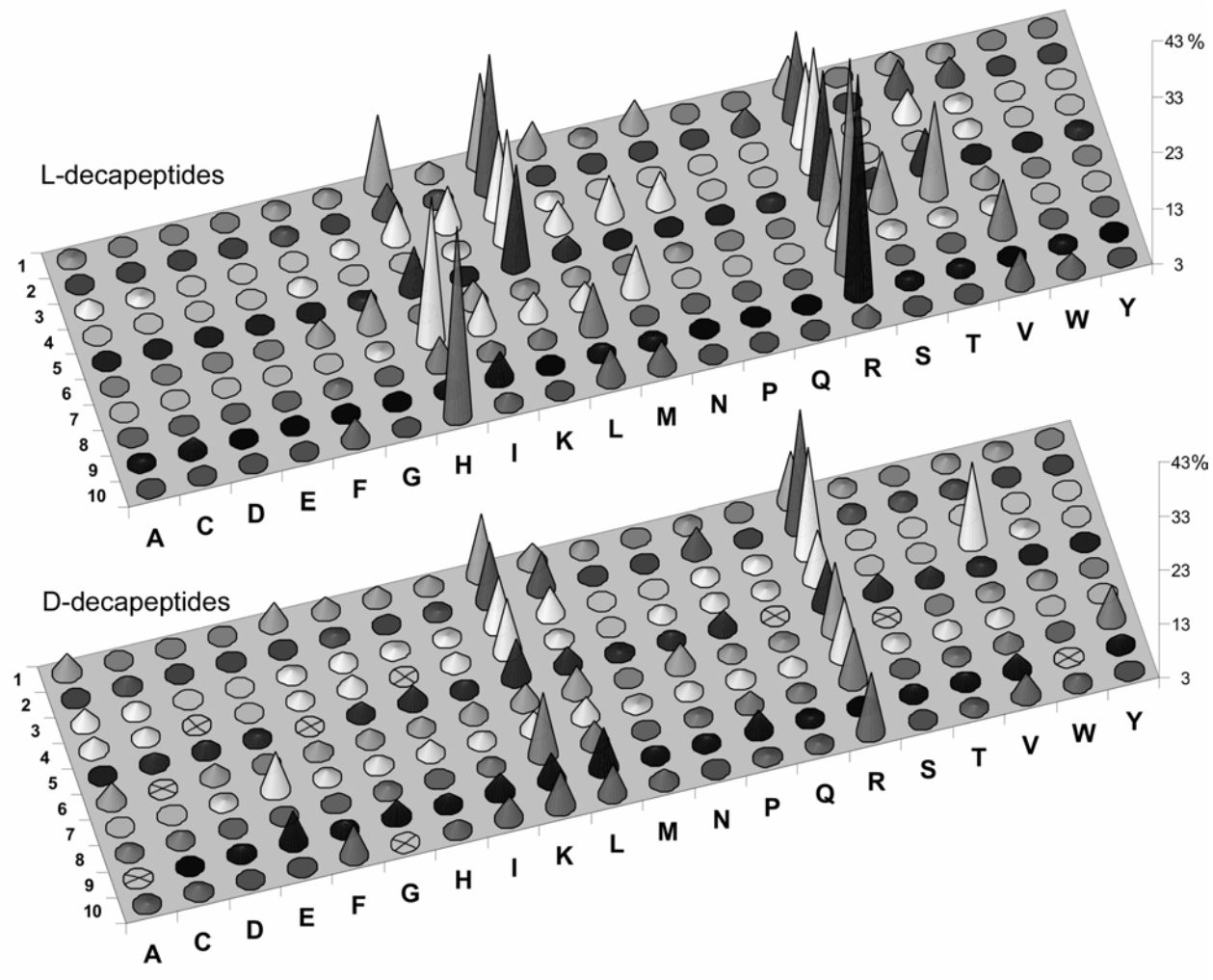

Figure 4

Kacprzak et al., 2004

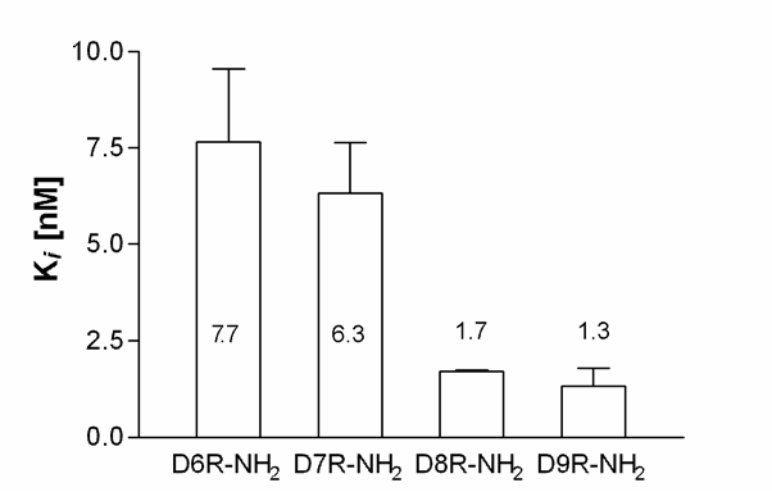

Figure 5

Kacprzak et al., 2004

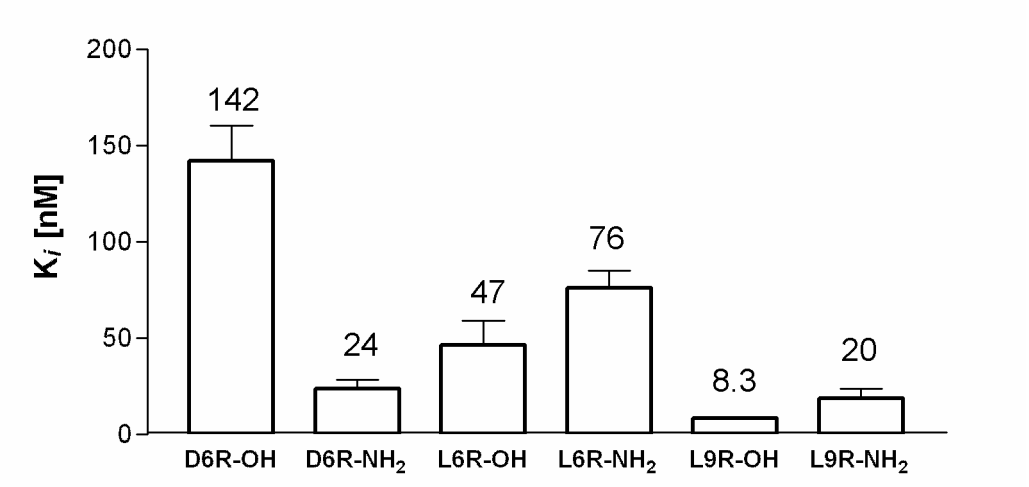

Figure 6

Kacprzak et al., 2004